

Selenium-Engineered Covalent Organic Frameworks for High-Efficiency and Long-Acting Cancer Therapy

Xiuyan Wan,[‡] Tong Wu,[‡] Liqun Song, Wei Pan, Na Li, and Bo Tang**

College of Chemistry, Chemical Engineering and Materials Science, Key Laboratory of Molecular and Nano Probes, Ministry of Education, Collaborative Innovation Center of Functionalized Probes for Chemical Imaging in Universities of Shandong, Institute of Molecular and Nano Science, Shandong Normal University, Jinan 250014, P. R. China

*lina@sdu.edu.cn (N. Li)

*tangb@sdu.edu.cn (B. Tang)

Table of Contents

EXPERIMENTAL SECTION.....	S-3
Materials and reagents.....	S-3
Instruments.....	S-3
Preparation of COF-PEL.....	S-4
Preparation of Se@COF.....	S-4
Synthesis of aldehyde group modified PEG (OHC-PEG-CHO).....	S-4
Modification CHO-PEG of Se@COF.....	S-5
Synthesis of Se@COF@IR808.....	S-5
Verification of the generation of ¹ O ₂ in vitro.....	S-5
Cell culture.....	S-5
Detection of ROS in cells.....	S-5
Detection of mitochondrial membrane potential ($\Delta\psi_m$).....	S-6
MTT staining assays.....	S-6
Live/Dead Cell Staining Assays.....	S-7
Detection of cell Apoptosis.....	S-7
Tumor Model Establishment.....	S-7
<i>In vivo</i> therapeutic effect of the COFs.....	S-8
<i>In vivo</i> Fluorescence Imaging.....	S-8
Blood biochemical parameters analysis.....	S-9
SUPPORTING FIGURES.....	S-10
Figure S1. The FT-IR spectra of COF.....	S-10
Figure S2. DLS size distribution of COF.....	S-11
Figure S3. DLS size distribution of Se@COF.....	S-12
Figure S4. The EDX spectrum of Se@COF-PEG.....	S-13
Figure S5. DLS size distribution of Se@COF-PEG.....	S-14
Figure S6. The absorbance spectra of ABMD solutions with different treatments.....	S-15
Table S1. The absorbance value of formazan solution at 570 nm corresponding to Figure 3a.....	S-16
Table S2. The absorbance value of formazan solution at 570 nm corresponding to Figure 3d.....	S-17
Figure S7. CLSM images of 4T1 cells to detect ROS production.....	S-18
Figure S8. Live/dead cell staining assay to visualize cell viabilities of 4T1 cells.....	S-19
Figure S9. Photographs of the tumor dissection with various intratumorally injected treatments.....	S-20
Figure S10. Time-dependent tumor growth profiles with various intratumorally injected treatments.....	S-21
Figure S11. Photographs of the representative mice with various intratumorally injected treatments.....	S-22
Figure S12. H&E-stained images of tumor slice with various intratumorally injected treatments.....	S-23
Figure S13. DLS measured size of Se@COF-PEG with different treatments for 24 h.....	S-24
Figure S14. TCPP release of Se@COF-PEG with PBS for different times.....	S-25
Figure S15. Relative fluorescence signal in tumor of Figure 5a.....	S-26
Figure S16. H&E-stained images of tumor slice with various intratumorally intravenously treatments.....	S-27
Figure S17. Body weight changes of mice intravenously injected with different treatments.....	S-28
Figure S18. Body weight changes of mice intratumorally injected with different treatment.....	S-29
Figure S19. H&E staining of the five major organs intravenously injected with different treatments.....	S-30
Figure S20. H&E staining of the five major organs intratumorally injected with different treatments.....	S-31
Figure S21. Blood biochemical parameters after intravenously injected with different treatments.....	S-32
Figure S22. Blood biochemical parameters after intratumorally injected with different treatments.....	S-33

EXPERIMENTAL SECTION

Materials and reagents. **Materials and reagents.** 2,5-dihydroxyterephthalaldehyde (DHa) and tetra (p-amino-phenyl) porphyrin (TAPP) were obtained from Changchun Third Party Pharmaceutical Technology Co. Ltd. Selenous acid (H_2SeO_3), 2', 7'- dichlorofluorescein diacetate (DCFH-DA), 3-(4, 5-dimethyl-thiazole-2-yl)-2, 5-diphenyltetrazolium bromide (MTT), 9, 10-anthracyl-bis(methylene)dimalonic acid (ABMD), 1,3-diphenylisobenzofuran (DPBF), Propidium iodide (PI), and Calcein acetoxymethyl ester (Calcein-AM) were purchased from Sigma Chemical Company. Polyethyleneimine (PEI) was purchased from Macklin Biochemical Technology Co. Ltd. (Shanghai, China). Polyvinylpyrrolidone (PVP) was purchased from Heowns Biochemical Technology Co., Ltd. (Tianjin, China). The experimental water used was Mill-Q secondary ultrapure water ($18.2 \text{ M}\Omega \cdot \text{cm}^{-1}$). All the other chemical reagents were of analytical grade and used without further purification. The mouse mammary carcinoma cells (4T1 cell) were purchased from AOLU Biological Technology Co. Ltd. (Shanghai, China). TC-1 cells were purchased from Shanghai AOLU Biological Technology Co. Ltd. (Shanghai, China). Fetal bovine serum (FBS) were purchased from Biological Industries (BIOIND).

Instruments. Transmission electron microscopy (TEM, JEM-2100) was employed to characterize the morphologies of the nanoreactors. The crystal structure of the nanoreactors was verified by powder X-ray diffraction (PXRD, Bruker D8, Germany). Zeta potential was performed on a Malvern Zeta Sizer Nano (Malvern Instruments). UV-vis spectroscopy was achieved with U-4100 UV-visible Spectrophotometer (HITACHI, Japan). Fourier infrared spectrometer (Nicolet iS50 FT-IR) was used to characterize the infrared spectrum. All pH measurements were performed with a digital pH-meter (pH-3e, LeiCi, China). The absorbance was measured in a microplate reader (RT 6000, Rayto, USA) for the MTT assay. Confocal

fluorescence imaging studies were performed using a TCS SP8 confocal laser scanning microscope (Leica, Germany). *In vivo* fluorescence images were captured using live animal imaging system (IVIS Lumina III, US).

Preparation of COF-PEI. Considering the negative charge of COF, PEI was used to modify COF for obtaining a highly positive charge, making SeO_3^{2-} absorbed on the surface of COF via electrostatic interaction. Firstly, COF (1 mg) was dispersed into aqueous (5 mL) solution containing PEI (10 mg) and then stirred for 6 h. The mixture solution was centrifuged and dispersed into aqueous solution.

Preparation of Se@COF. Se@COF were designed and synthesized via the PVP-mediated in situ synthesis strategy. Briefly, 1mg of COF-PEI was dispersed into 5 ml aqueous solution containing 1.2 mg H_2SeO_3 and 0.36 mg PVP and stirred for 1h. Then, 2.4 mg ascorbic acid was added slowly into the above solution under vigorously stirring. After 3h, the reaction mixture generates a red solution, suggesting the successfully complexation of Se NPs. After ultrasonic for 1h, the resulting solution was collected and washed with water for three times.

Synthesis of Aldehyde Group Modified PEG (OHC-PEG-CHO). Firstly, PEG (10 g, 5 mmol), 4-carboxybenzaldehyde (2.25 g, 15mmol), EDC·HCl (9.585 g, 50 mmol) and DMAP (0.244 g, 2 mmol) were dissolved in 150 mL dichloromethane (DCM) and stirred for 48 h at 25 °C. The obtained solution was concentrated by rotary evaporator, and washed for five times with saturated NaCl solution and another three times with 5% NaCl solution respectively. Subsequently, the organic layer was collected and 50~100 g anhydrous magnesium sulfate as dehydration agent was added and stood for about 12 h. After filtration, the filtrate was

concentrated and deposited twice with excess diethyl ether. The final product was dried under vacuum at room temperature overnight.

Modification CHO-PEG of COF-SeNPs. Due to the rich amino on the surface of COF, the modification of CHO-PEG could easily achieve through aldimine condensation. 2 mg Se@COF was dispersed into 5 ml aqueous solution and then stirred for 1h. Se@COF-PEG can be obtained after centrifugation.

Synthesis of Se@COF@IR808. 1 mg Se@COF-PEG/Se@COF were dispersed into in 2 mL aqueous solution and 20 μ L of IR808 solution (10 mg/mL) was added into the solution. Then the solution was stirred for 12 h and the product Se@COF-PEG/Se@COF@IR808 was obtained after centrifugation.

Verification of the generation of $^1\text{O}_2$ in vitro. $^1\text{O}_2$: The generation of $^1\text{O}_2$ was verified by employing the $^1\text{O}_2$ -specific molecular probe ABMD and determined via the UV-vis spectra. COF and COF-Se (50 $\mu\text{g}\cdot\text{mL}^{-1}$) was added to the ABMD (0.1 mM) aqueous solution and irradiated by a 635 nm laser (0.2 $\text{W}\cdot\text{cm}^{-2}$, 10 min). ABMD aqueous solution was set up as the control group.

Cell culture. 4T1 and TC-1 cells used in the experiments were cultured in RPMI 1640 with 10% fetal bovine serum (FBS) and 100 U/mL of 1% penicillin/ streptomycin and maintained at 37 $^\circ\text{C}$ in an incubator with a humidified 5% CO_2 /95% air atmosphere.

Detection of ROS in cells. Five groups of 4T-1 cells were seeded in a confocal dish and incubated with COF (75 $\mu\text{g}/\text{mL}$), COF-Se (75 $\mu\text{g}/\text{mL}$) for 4 h in 5% CO_2 at 37 $^\circ\text{C}$, and then washed with PBS for three times. After incubated with DCFH-DA (2 μM) for 20 min, 4T1 cells

were imaged by fluorescence imaging with 488 nm excitation. For laser groups, the cells were first incubated with DCFH-DA for 10 min and were irradiated with 635 nm laser at $0.2 \text{ W}\cdot\text{cm}^{-2}$ for 10 min. Then the cells were also examined with CLSM with the same parameters.

Detection of mitochondrial membrane potential ($\Delta\Psi_m$). Four groups of 4T1 cells were incubated with COF ($75 \mu\text{g}/\text{mL}$), COF-Se ($75 \mu\text{g}/\text{mL}$) for 4 h and the laser groups were subjected to 635 nm for 10 min. Then, the cells were incubated with rhodamine 123 ($5 \mu\text{g}/\text{mL}$) for 15 min. Confocal images of rhodamine 123-stained cells were obtained by excitation of the samples at 488 nm (emission = 500-550 nm).

MTT assays. (1) In Vitro Cytotoxicity. The 4T1 cells were seeded into a 96-well plates and cultured for 24 h. Five groups of cells were performed as follows: control, COF-PEG, Se@COF, COF-PEG+ Laser, Se@COF-PEG + Laser. The culture medium was then replaced with $150 \mu\text{L}$ of freshly complete medium containing different concentration of nanoparticles ($25, 50, 75$ and $100 \mu\text{g}\cdot\text{mL}^{-1}$) and cultured for 4 hours follow by washing the cells with PBS buffer to remove the excess materials. The laser groups were treated irradiation with the 635 nm laser at $0.2 \text{ W}\cdot\text{cm}^{-2}$ for 10 min. Then, the cells were cultured for another 12 h and $150 \mu\text{L}$ of MTT solution ($0.5 \text{ mg}\cdot\text{mL}^{-1}$) was then added to each well. After 4 h of treatment, the MTT solution was discarded, and $150 \mu\text{L}$ of dimethyl sulfoxide (DMSO) was added to dissolve formazan crystals. Finally, the absorbance was measured at 490 nm using a microplate reader. Then the cell viabilities were calculated based on the following equation: Cell viability = $A_n/A_{\text{PBS}} \times 100\%$. (2) To verify the time-dependent cancer cell growth inhibitory effect of different treatments, the cells were seeded into a 96-well plates and cultured with COF-PEG, Se@COF-PEG ($75 \mu\text{g}\cdot\text{mL}^{-1}$). After 4 h incubation, the cells were washed with PBS buffer to remove the excess materials. The laser groups were treated irradiation with the 635 nm laser at $0.2 \text{ W}\cdot\text{cm}^{-2}$ for 10 min and

after another 12h incubation, the cell viabilities were evaluated with MTT assay. The above cell treatment was regarded as one treatment of the cells, and then two, three and four successive treatments were performed to verify the photodynamic resistance of the cells. (3) To evaluate the influence of hypoxia conditions on different treatments, 4T1 cells were incubated in 96-well plates and cultured for 24h under anaerobic conditions. The cells were divided into four groups: control, COF-PEG + Laser, Se@COF-PEG, Se@COF-PEG + Laser. The concentration of the nanoparticles was $50 \mu\text{g}\cdot\text{mL}^{-1}$. After incubated in anaerobic conditions for 4 h, the laser groups were treated irradiation with the 635 nm laser at $0.2 \text{ W}\cdot\text{cm}^{-2}$ for 10 min and after another 12h incubation, the cell viabilities were evaluated with MTT assay.

Live/Dead Cell Staining Assays. For further evaluating the therapeutic effects of different materials on 4T1 cells, live/dead dual staining assays was used. 4T1 cells were seeded onto glass-bottom dishes for 24 h. Then, the cells were incubated with sample solution for 4 h without laser irradiation or with laser irradiation ($0.2 \text{ W}\cdot\text{cm}^{-2}$, 10 min). After 12 h incubation, the culture medium was discarded, and cells were washed three times with PBS. Then the cells were stained with calcein-AM (20 nM) and PI ($4\mu\text{M}$) solution in PBS buffer solution for 20 min. Finally, the cells were washed three times with PBS and imaged by confocal fluorescence imaging. Green fluorescence of calcein-AM was excited at 488 nm and detected with a 500–550 nm bandpass filter. Red fluorescence of PI was excited at 633 nm and detected with a 660–710 nm bandpass filter.

Detection of cell Apoptosis. Cell apoptosis was evaluated by flow cytometry. The cells were divided into five groups: control, COF-PEG, Se@COF-PEG, COF-PEG + Laser, Se@COF-PEG + Laser ($75 \mu\text{g}/\text{mL}$). After 24 h incubation, the cells were labeled with annexin V–FITC and PI and analyzed by flow cytometry.

Tumor Model Establishment. All animal procedures were performed in accordance with the Principles of Laboratory Animal Care (People's Republic of China) and were approved by the Animal Care and Use Committee of Shandong Normal University (Jinan, China). Female nude mice (4-6 weeks old, ~20 g) were housed under normal conditions with 12 h light and dark cycles and given access to food and water ad libitum. The 4T1 xenograft tumor model was used as an example to evaluate the therapeutic effect. To this end, 1×10^7 4T1 cells in 100 μ L of serum-free RPMI 1640 medium were injected subcutaneously into the right axillary region of BALB/c mice. The mice were given different treatment, when the tumor size had reached approximately 80-100 mm³.

***In vivo* therapeutic effect of the COFs.** The 4T1 tumor-bearing BALB/c mice were randomly divided into five groups (n = 4 per group). (1) Control, (2) COF-PEG, (3) Se@COF-PEG, (4) COF-PEG+ Laser, (5) Se@COF-PEG + Laser. 50 μ L PBS, the dose was 4 mg·kg⁻¹ (in terms of the COF). After intravenous injection, the tumors were exposed to 635 nm laser irradiation for 10 min in laser groups at 24 h post-injection. After intratumor injection, the tumors were irradiated immediately. The tumor size and the body weights of the mice were measured every other day for 14 days (day 0, 2, 4, 6, 8, 10, 12 and 14). The tumor volume (V) was determined by measuring length (L) and width (W), and calculated as $V = L \times W^2 / 2$.

***In Vivo* Fluorescence Imaging.** The tumor-bearing BALB/c mice were injected with Se@COF@IR808 or Se@COF-PEG@IR808 (4mg·kg⁻¹) via tail vein, and fluorescence imaging measurements were conducted at different time points (2, 6, 10, 12, 24, and 96 h).

Histopathological analysis. Tumor bearing mice were intravenously or intratumorally injected with PBS, COF-PEG, Se@COF-PEG (4mg/kg). The H&E staining of the organs (heart, liver,

spleen, lung, and kidney) were tested at 14 days post-injection and the tumors were tested at 12 h after irradiation.

Blood biochemical parameters analysis. Normal mice were intravenously injected with PBS, COF-PEG, Se@COF-PEG (4 mg/kg), and the blood was collected for subsequent analysis at post 14 days intravenous or intratumor injection. The blood sample of mice was also collected from the retro-orbital plexus into a coagulation-promoting tube, and then centrifuged at 3000 rpm 4 °C for 20 min to obtain plasma samples. The serum biochemical parameters including alanine aminotransferase (ALT), aspartate aminotransferase (AST), blood urea nitrogen (BUN) and creatinine (CRE) were tested using the automatic biochemical analyzer.

SUPPORTING FIGURES

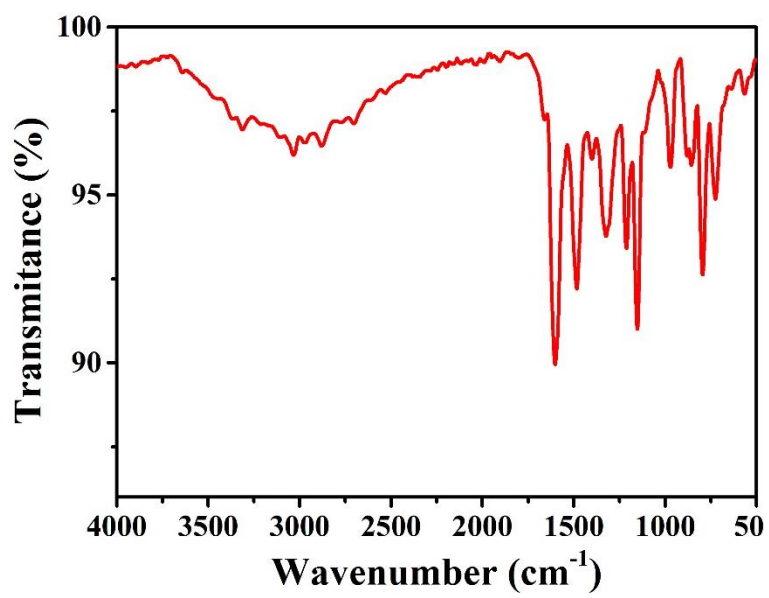


Figure S1. The FT-IR spectra of COF.

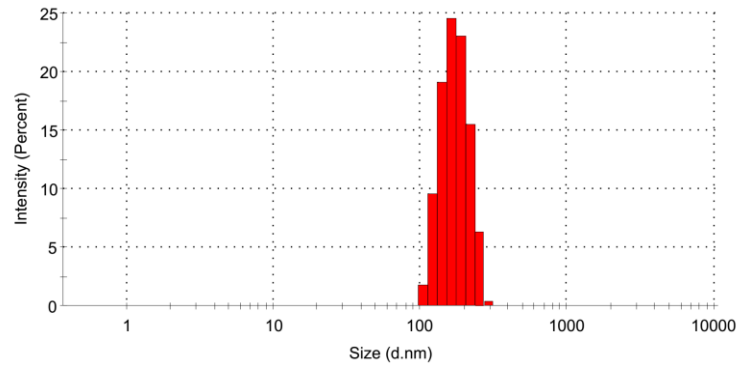


Figure S2. DLS size distribution of COF.

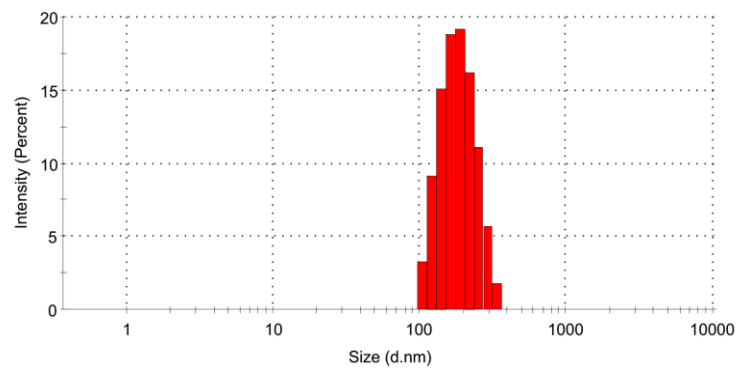


Figure S3. DLS size distribution of Se@COF.

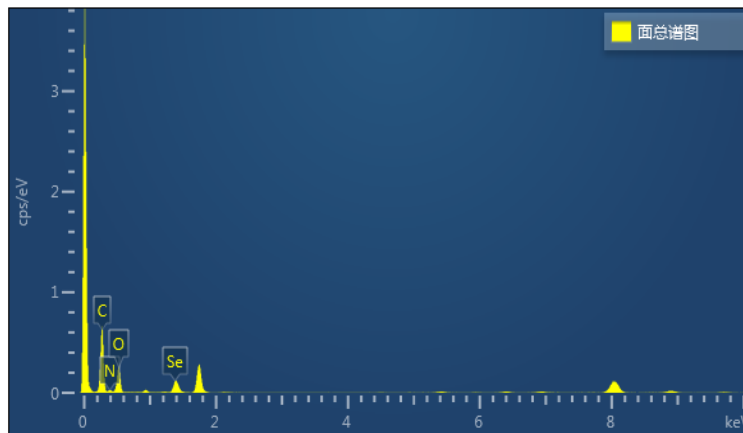


Figure S4. The EDX spectrum of Se@COF-PEG.

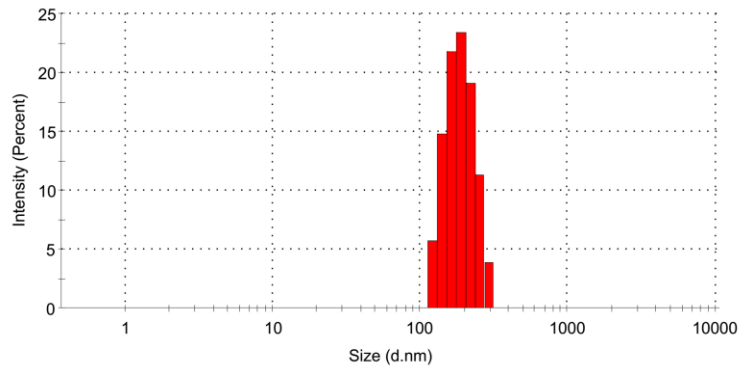


Figure S5. DLS size distribution of Se@COF-PEG.

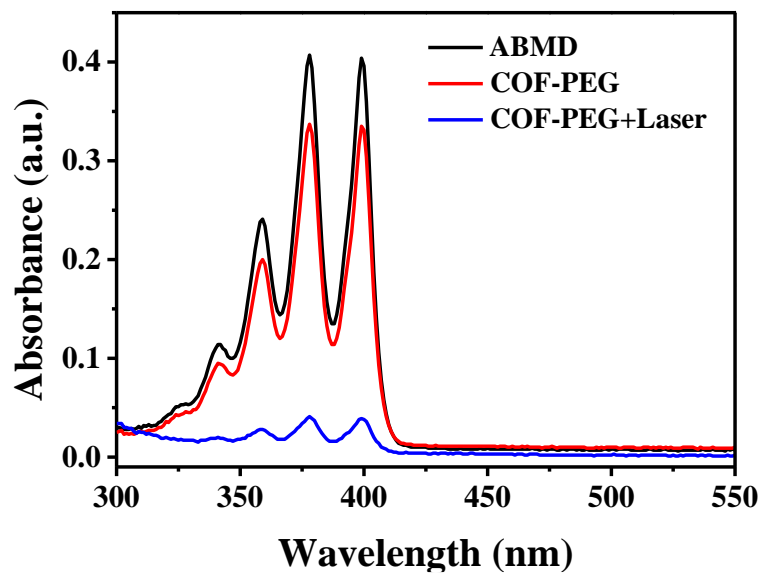


Figure S6. The absorbance spectra of ABMD solutions with different treatments.

Table S1. The absorbance value of formazan solution at 490 nm corresponding to Figure 3a.

$\bar{A}_{\text{absorbance}}$ / concentration	25 $\mu\text{g/ml}$	50 $\mu\text{g/ml}$	75 $\mu\text{g/ml}$	100 $\mu\text{g/ml}$
groups				
PBS	1.596 (± 0.05409)			
COF-PEG	1.526 (± 0.02837)	1.487 (± 0.01649)	1.456 (± 0.04185)	1.411 (± 0.02895)
Se@COF-PEG	1.294 (± 0.05085)	1.254 (± 0.02189)	1.195 (± 0.07656)	1.132 (± 0.02120)
COF-PEG+Laser	1.037 (± 0.05192)	1.034 (± 0.04547)	0.870 (± 0.02414)	0.768 (± 0.02538)
Se@COF-PEG+Laser	0.840 (± 0.01711)	0.716 (± 0.05347)	0.588 (± 0.01316)	0.276 (± 0.00822)

Table S2. The absorbance value of formazan solution at 490 nm corresponding to Figure 3d.

\bar{A} absorbance time	groups	PBS	COF-PEG+Laser	Se@COF-PEG	Se@COF-PEG+Laser
Day1		1.237 (± 0.01654)	0.709 (± 0.02559)	0.988 (± 0.01548)	0.539 (± 0.08532)
Day2		1.415 (± 0.01513)	0.979 (± 0.05168)	1.090 (± 0.02549)	0.593 (± 0.02077)
Day3		1.788 (± 0.02267)	1.310 (± 0.04397)	1.328 (± 0.10049)	0.635 (± 0.00569)
Day4		2.946 (± 0.01177)	2.442 (± 0.03995)	2.111 (± 0.02683)	1.023 (± 0.01765)

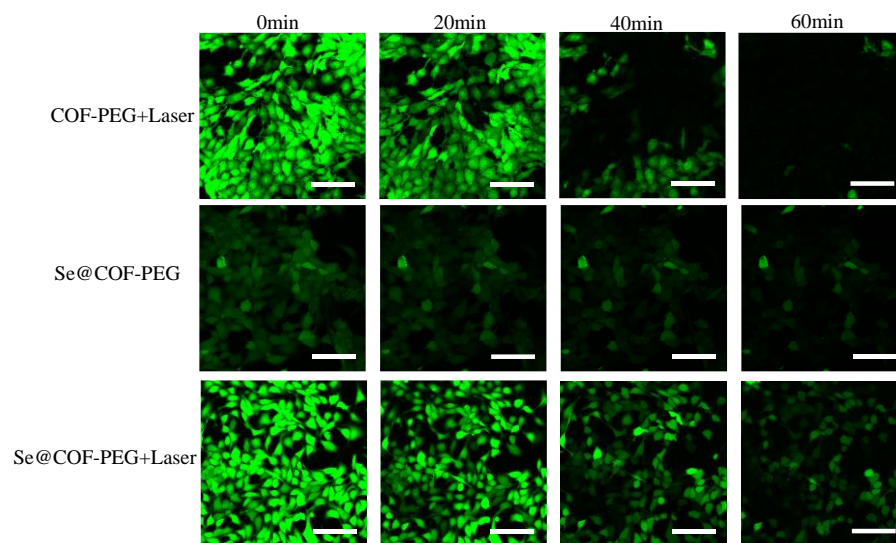


Figure S7. CLSM images of 4T1 cells with various treatments for different times to detect ROS production on account of DCF-DA fluorescent intensity.

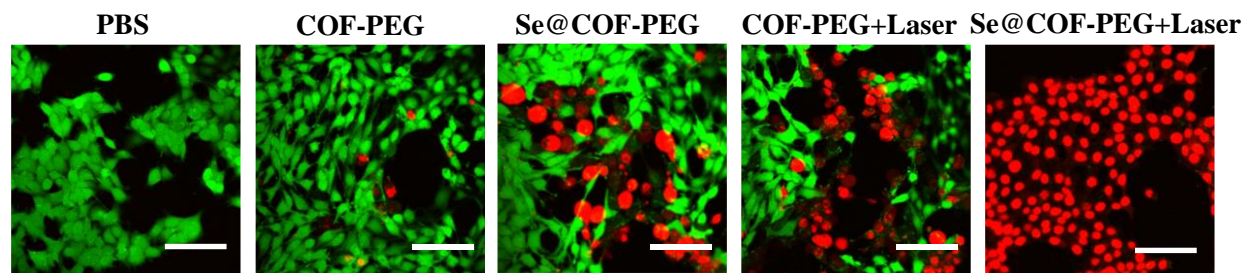


Figure S8. Live/dead cell staining assay to visualize cell viabilities of 4T1 cells under different treatments.

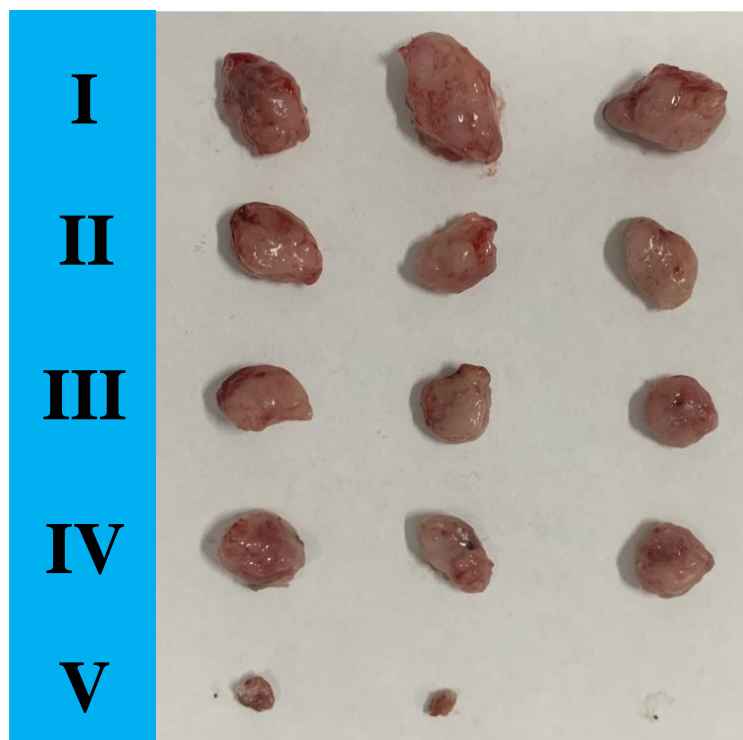


Figure S9. Photographs of the tumor dissection with various treatments (I: PBS; II: COF-PEG; III: COF-PEG+Laser; IV: Se@COF-PEG, V: Se@COF-PEG + Laser)

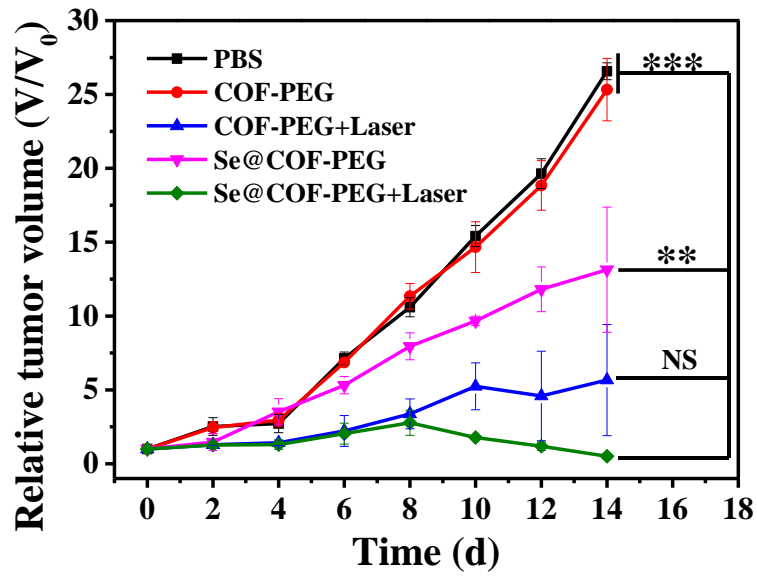


Figure S10. Time-dependent tumor growth profiles.

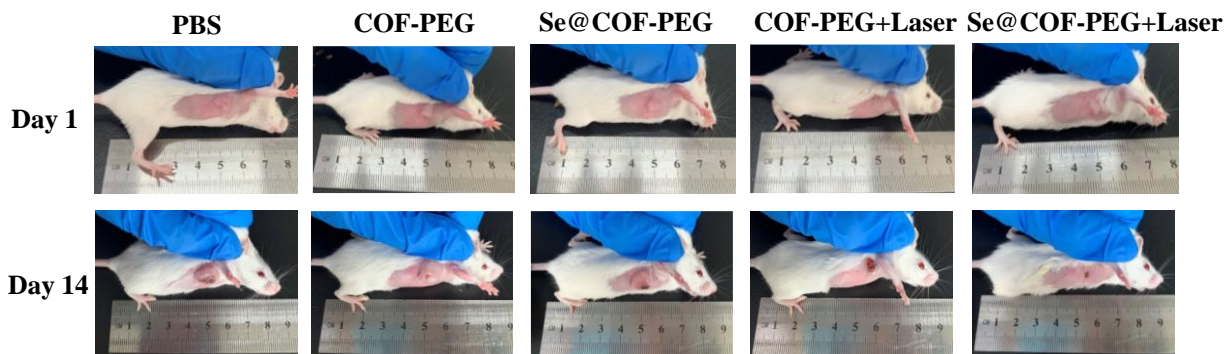


Figure S11. Photographs of the representative 4T1 tumor-bearing mice before treatments and on day 14 after the treatments.

As shown in Fig. S9–S11, no obvious anti-tumor effect was observed in PBS or COF-PEG without laser irradiation. The tumors of mice injected with COF-PEG together with being subjected to laser irradiation were suppressed for a short period of time, but then the tumor regrew aggressively, which confirmed that PDT by itself did not inhibit the tumor growth efficiently and in fact elicited tumor recurrence after some time. For mice not subjected to laser irradiation but injected with Se@COF-PEG, the tumor grew slowly but steadily, indicating the limited therapeutic efficacy of SeT by itself. In contrast, the synergistic treatment involving PDT with SeT clearly suppressed the tumor growth much more efficiently, and this tumor suppression was maintained during the whole therapeutic session without regrowth and recurrence.

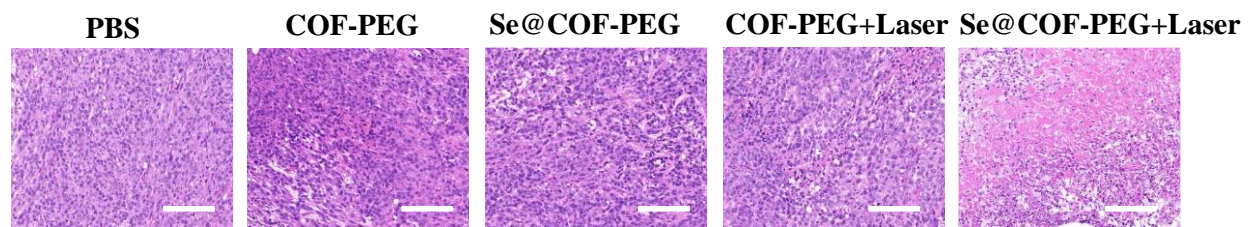


Figure S12. H&E-stained images of tumor slice with various treatments. Scale bars = 100 μm .

Hematoxylin and eosin (H&E) staining assay also revealed that the treatment of Se@COF-PEG under laser irradiation triggered the most serious damage to tumor tissue (Fig. S12, ESI[†]).

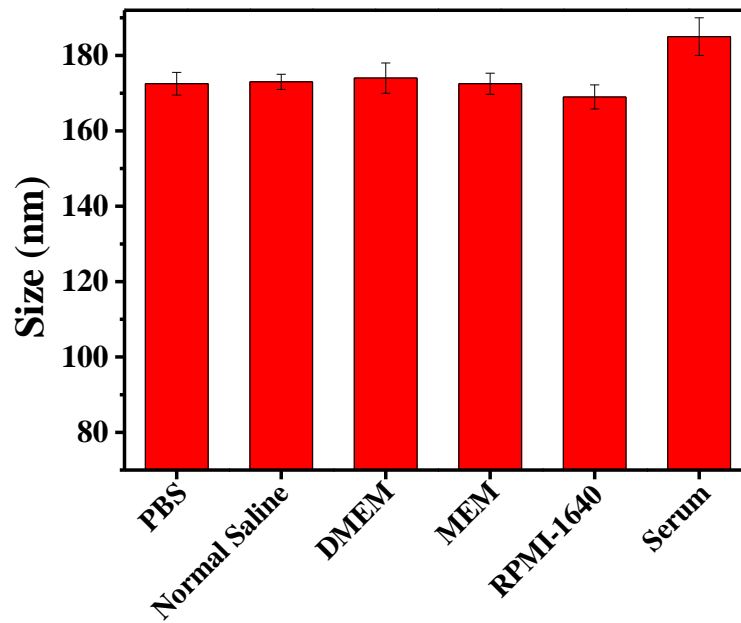


Figure S13. DLS size of Se@COF-PEG with different treatments for 24 h.

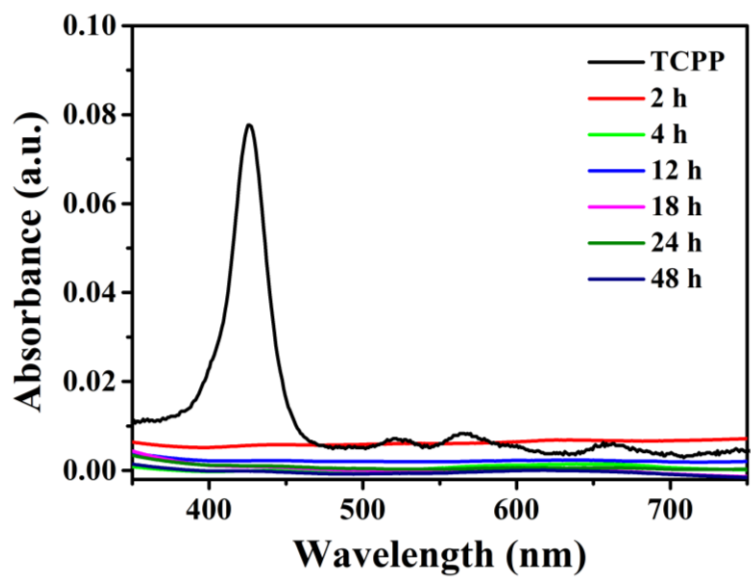


Figure S14. TCPP release of Se@COF-PEG treated with PBS for different times.

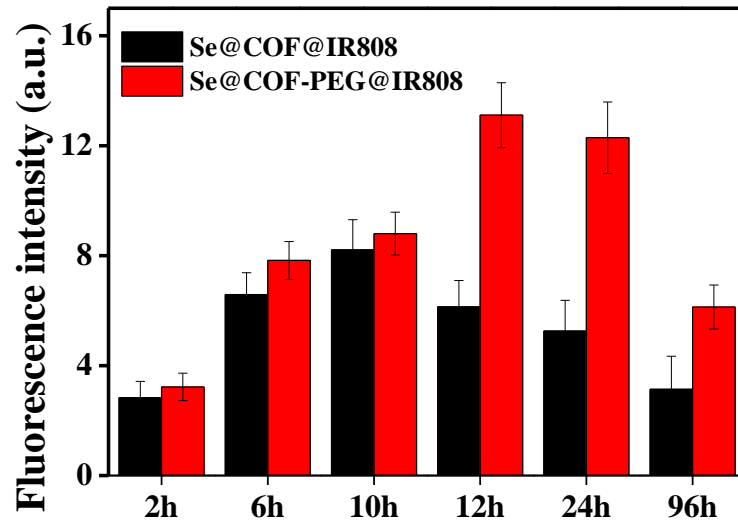


Figure S15. Relative fluorescence signal in tumor of Figure 5a at different time points of tumor bearing mice after intravenous injection of Se@COF@IR808 or Se@COF-PEG@IR808.

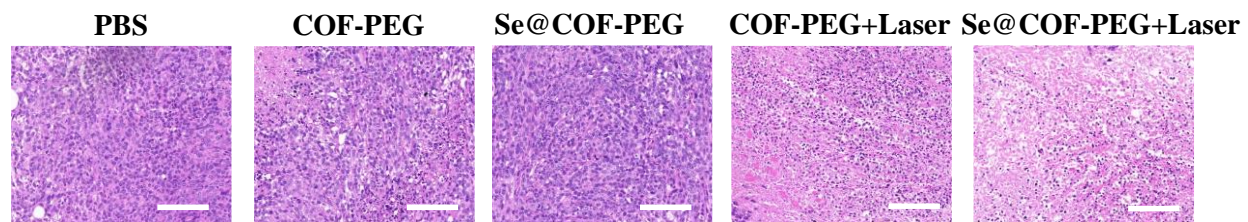


Figure S16. H&E-stained images of tumor slices for various treatments. Scale bar = 100 μm .

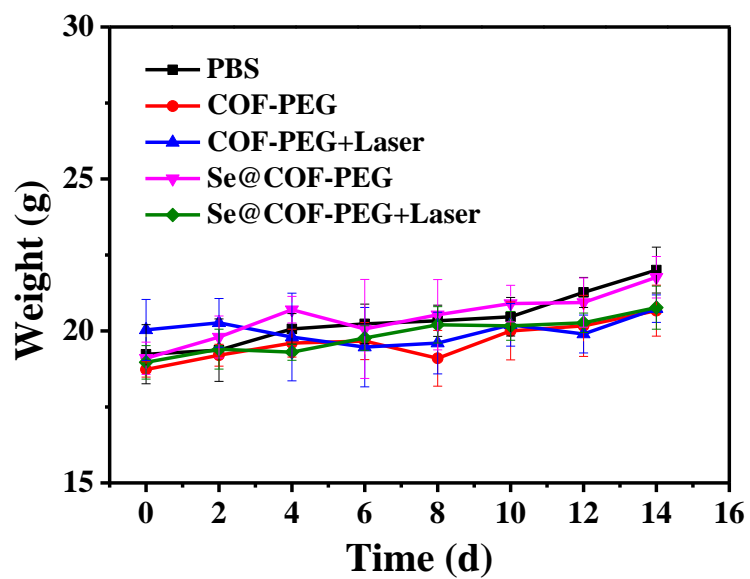


Figure S17. Body weight changes of mice intravenously injected with different treatments within 14 days.

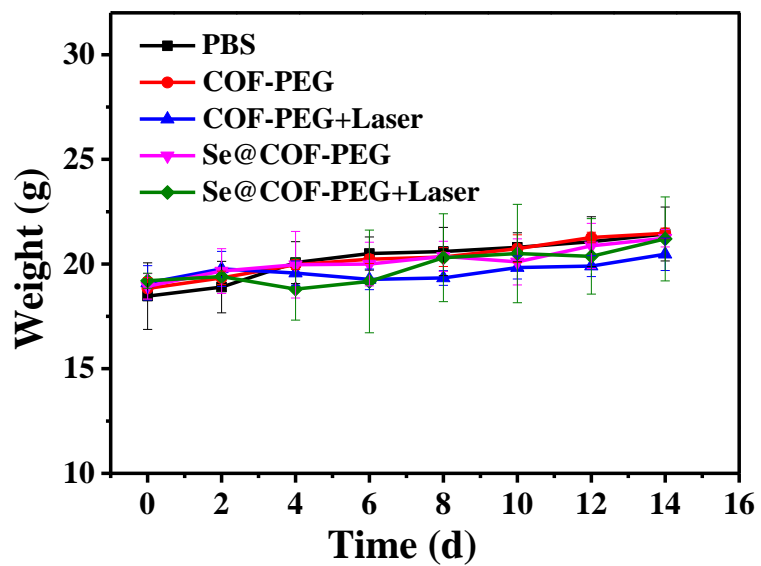


Figure S18. Body weight changes of mice intratumorally injected with different treatments within 14 days.

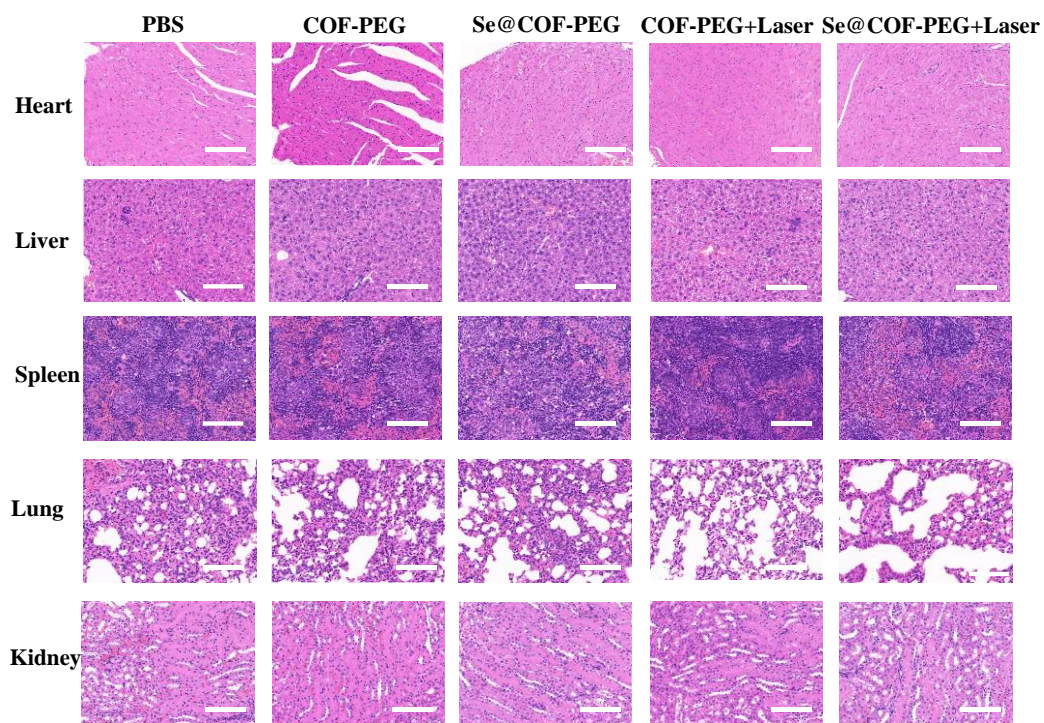


Figure S19. H&E staining of the five major organs (heart, liver, spleen, lung and kidney) intravenously injected with different treatments after 14 days. All scale bars are 100 μm .

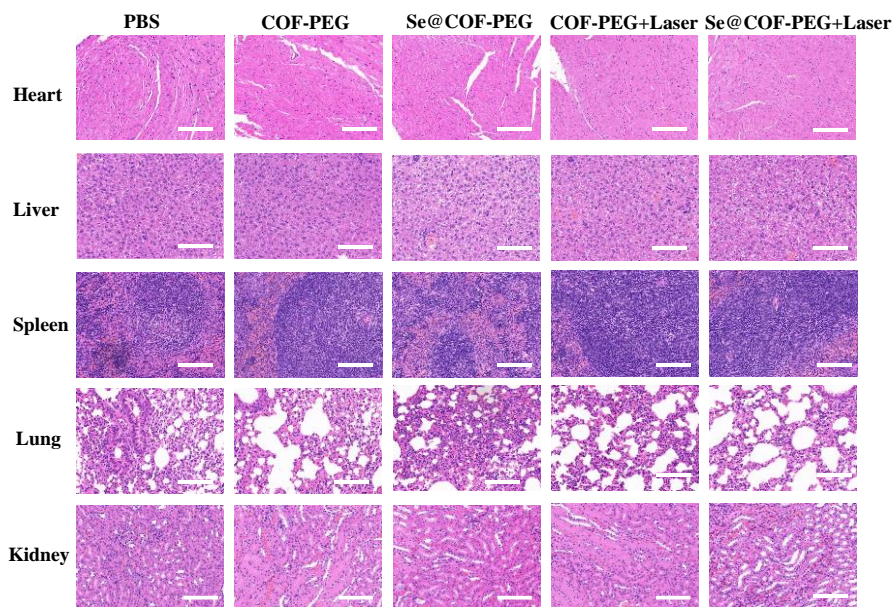


Figure S20. H&E staining of the five major organs (heart, liver, spleen, lung and kidney) intratumorally injected with different treatments after 14 days. All scale bars are 100 μm .

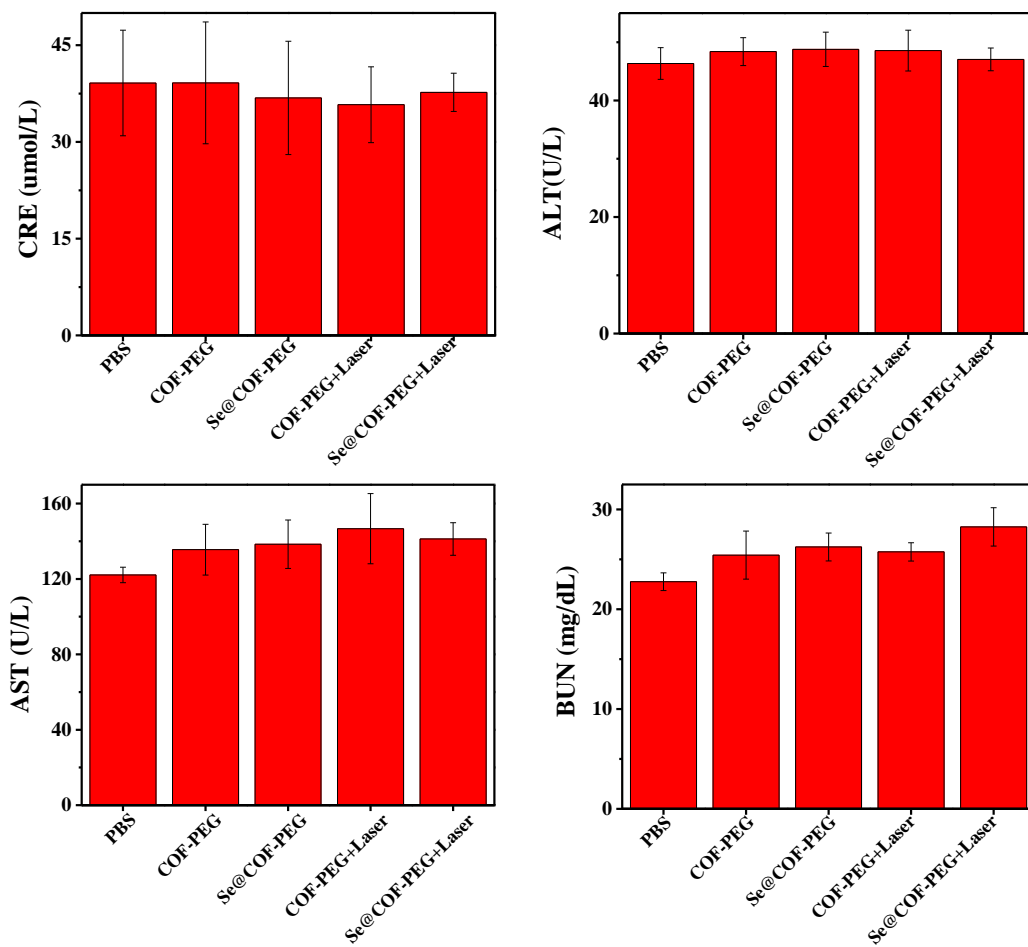


Figure S21. Blood biochemical parameters after intravenously injected with different treatments for 14 days. The blood was collected for detection of the levels of CRE, ALT, AST, and BUN.

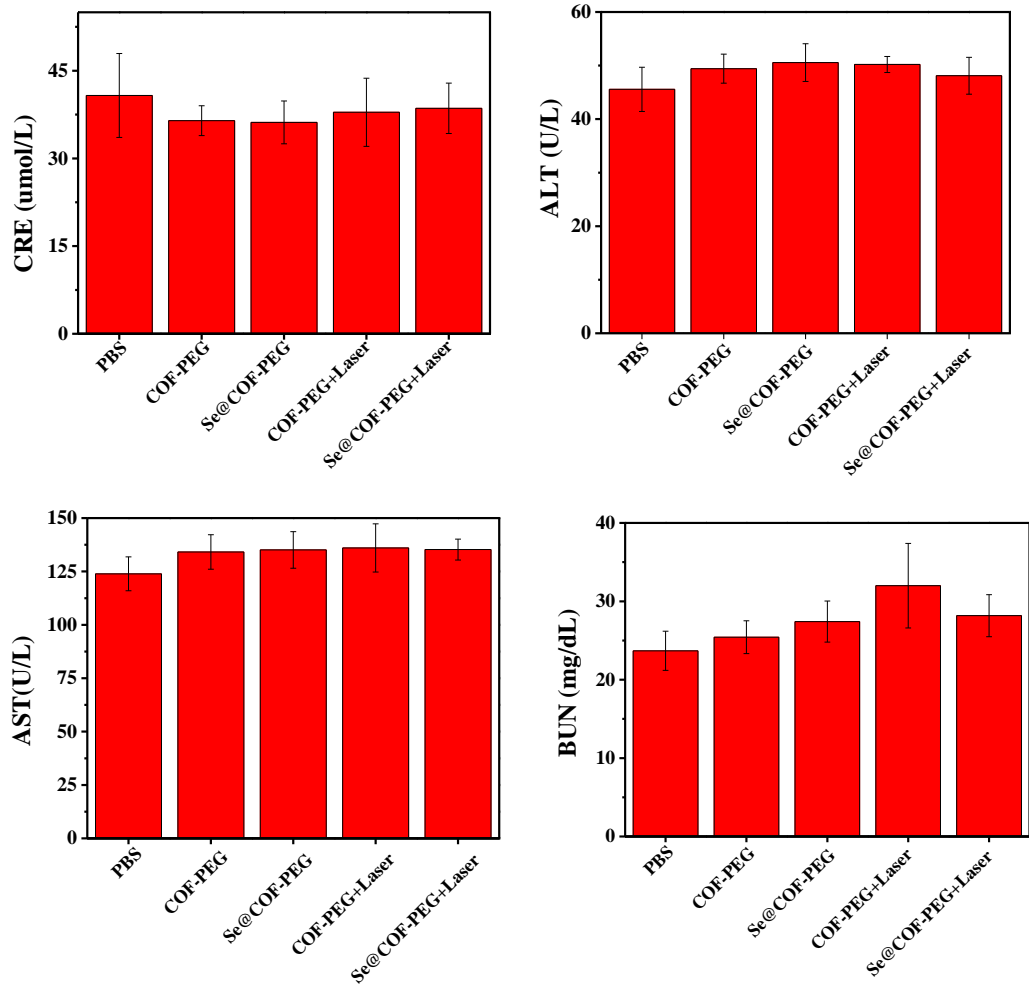


Figure S22. Blood biochemical parameters after intratumorally injected with different treatments for 14 days. The blood was collected for detection of the levels of CRE, ALT, AST, and BUN.